Hindawi Publishing Corporation
EURASIP Journal on Wireless Communications and Networking
Volume 2008, Article ID 273018, 9 pages
doi:10.1155/2008/273018

Research Article

Capacity of Time-Hopping PPM and PAM UWB Multiple Access Communications over Indoor Fading Channels

Hao Zhang[1] and T. Aaron Gulliver[2]

[1] *Department of Electrical Engineering, Ocean University of China, 5 Yushan Road, Qingdao 266003, China*
[2] *Department of Electrical & Computer Engineering, University of Victoria, P.O. Box 3055, STN CSC, Victoria, BC, Canada V8S 4W9*

Correspondence should be addressed to Hao Zhang, zhanghao@ouc.edu.cn

Received 27 June 2007; Revised 10 October 2007; Accepted 10 February 2008

Recommended by Weidong Xiang

The capacity of time-hopping pulse position modulation (PPM) and pulse amplitude modulation (PAM) for an ultra-wideband (UWB) communication system is investigated based on the multipath fading statistics of UWB indoor wireless channels. A frequency-selective fading channel is considered for both single-user and multiple-user UWB wireless systems. A Gaussian approximation based on the single-user results is used to derive the multiple access capacity. Capacity expressions are derived from a signal-to-noise-ratio (SNR) perspective for various fading environments. The capacity expressions are verified via Monte Carlo simulation.

1. INTRODUCTION

Ultra-wideband (UWB) [1] communication systems employ ultrashort impulses to transmit information which spreads the signal energy over a very wide frequency spectrum of several GHz. Multipath fading is one of the major challenges faced by UWB systems. The statistics of narrowband indoor wireless channels have been extensively investigated and several widely accepted channel models have been developed. However, narrowband models are inadequate for the characterization of UWB channels because of their extremely large transmission bandwidth and nanosecond path delay difference resolvable paths. Considering these characteristics, the so-called POCA-NAZU model and the stochastic tapped-delay-line (STDL) propagation model have been proposed for UWB indoor wireless channels [2, 3]. The parameters of the STDL model were obtained from channel measurements. It was shown that the Nakagami distribution is a better fit for the indoor wireless magnitude statistics rather than the distributions typically used in narrowband systems. Recently, the IEEE 802.15.4a group presented a comprehensive study of the UWB channel over the frequency range 2–10 GHz for indoor residential, indoor office, industrial, outdoor, and open outdoor environments [4]. It was suggested that small-scale fading be added based on the well-known Saleh-Valenzuela model. A list of parameters for different environments was also presented in [4]. Although the channel model presented in [4] describes the UWB indoor channel in more detail than the STDL model, it is difficult to use for capacity and performance analysis because of its complexity. In addition, it is not suitable for deriving general results which can be very useful to system designers. Therefore to facilitate and simplify the analysis, we employ the STDL model in this paper to study the capacity of a UWB system with PPM and PAM over indoor fading channels.

Extensive research has been conducted on the capacity of UWB systems in both AWGN and fading channels. In [5, 6], the channel capacity of UWB systems with M-ary pulse position modulation (PPM) is examined, and this is extended to biorthogonal PPM (BPPM) and pulse position amplitude modulation (PPAM) in [7, 8]. PPM and PAM with receive diversity are considered in [9]. However, these results are based on the assumption of an additive white Gaussian noise (AWGN) channel without considering multipath fading. In the following sections, we extend the analysis in [7–9] to derive the capacity of a UWB PPM and PAM system over indoor fading channels for both single and multiple user environments from a signal-to-noise ratio (SNR) perspective.

The rest of the paper is organized as follows. In Section 2, the time-hopping PPM and PAM UWB systems are introduced and a statistical model for the UWB indoor multipath channel is described. Section 3 presents the capacity analysis of PPM and PAM UWB systems over indoor fading channels with a single user. The discussion also covers frequency flat fading channels. The relationship between reliable communication distance and channel capacity subject to FCC Part 15 rules is given. The multiple access capacity of PPM and PAM UWB systems is analyzed in Section 4 via a Gaussian approximation. Numerical results are presented in Section 5 for the capacity over indoor fading channels. Finally, some conclusions are given in Section 6.

2. SIGNAL CONSTRUCTION AND STATISTICAL MODEL FOR MULTIPATH FADING UWB INDOOR CHANNELS

2.1. Signal construction and system model

A typical time-hopping format for the output of the kth user in a UWB system is given by [7]

$$s^{(k)}(t) = \sum_{j=-\infty}^{\infty} A^{(k)}_{d^{(k)}_{\lfloor j/N_s \rfloor}} q\left(t - jT_f - c_j^{(k)} T_c - \delta_{d^{(k)}_{\lfloor j/N_s \rfloor}}\right), \quad (1)$$

where $A^{(k)}$ is the signal amplitude, $q(t)$ represents the transmitted impulse waveform that nominally begins at time zero at the transmitter, and the quantities associated with (k) are transmitter dependent. T_f is the frame time, which is typically a hundred to a thousand times the impulse width resulting in a signal with a very low duty cycle. Each frame is divided into N_h time slots with duration T_c. The pulse shift pattern $c_j^{(k)}$, $0 \le c_j^{(k)} < N_h$ (also called the time-hopping sequence), is pseudorandom with period T_c. This provides an additional shift in order to avoid catastrophic collisions due to multiple access interference. The sequence d is the data stream generated by the kth source after channel coding, and δ is the additional time shift utilized by the N-ary pulse position modulation. If $N_s > 1$, a repetition code is introduced, that is, N_s pulses are used for the transmission of the same information symbol.

For M-ary PPM, we have constant unit signal amplitude, that is, $A^{(k)}_{d^{(k)}_{\lfloor j/N_s \rfloor}} = 1$, so (1) can be written as

$$s^{(k)}(t) = \sum_{j=-\infty}^{\infty} q\left(t - jT_f - c_j^{(k)} T_c - \delta_{d^{(k)}_{\lfloor j/N_s \rfloor}}\right). \quad (2)$$

For M-ary PAM, we have no additional modulation time shift, that is, $\delta_{d^{(k)}_{\lfloor j/N_s \rfloor}} = 0$. The normalized amplitude is defined as $A_m = (2m - 1 - M)\sqrt{E_g}$, $E_g = 3E_{\text{av}}/(M^2 - 1)$, $1 \le m \le M$, where E_{av} is the average energy of the signal. Equation (1) can then be written as

$$s^{(k)}(t) = \sum_{j=-\infty}^{\infty} A_{d^{(k)}_{\lfloor j/N_s \rfloor}} q(t - jT_f - c_j^{(k)} T_c). \quad (3)$$

The received signal over an additive white Gaussian noise (AWGN) channel can be modeled as the derivative of the transmitted pulses assuming propagation in free space [9]. Thus the received signal over indoor fading channels can be modeled as

$$\begin{aligned} r(t) &= \sum_{l=1}^{L} \sum_{k=1}^{K} h_{lk}(t) \left(s^{(k)}(t)\right)' + w(t) \\ &= \sum_{l=1}^{L} \sum_{k=1}^{K} \left(h_{lk}(t) \sum_{j=-\infty}^{\infty} A^{(k)}_{d^{(k)}_{\lfloor j/N_s \rfloor}} p\left(t - jT_f - c_j^{(k)} T_c - \delta_{d^{(k)}_{\lfloor j/N_s \rfloor}}\right) \right) + w(t), \end{aligned} \quad (4)$$

where $w(t)$ is AWGN with double-sided power spectral density N_o, K is the number of simultaneous active users, $p(t)$ is the received pulse waveform, L is the receive diversity order, that is, the number of resolvable paths in the case of a single-input single-output (SISO) system, and $h(t)$ is the time-varying attenuation. For an AWGN channel, if only one user is present, the optimal receiver for PPM is a bank of M correlation receivers followed by a detector. When more than one link is active in the multiple-access system, the optimal PPM receiver has a complex structure that takes advantage of all receiver knowledge regarding the characteristics of the multiple-access interference (MAI) [10]. However, for simplicity, an M-ary correlation receiver is typically used even when there is more than one active user. For PAM, only one correlation receiver is required for both the single user and multiuser cases. The receivers used for an AWGN channel can also be applied to multipath fading channels subject to the channel state information being fully available to the receiver for equalization.

2.2. Statistical model for the UMB indoor wireless multipath fading channel

Due to the ultrashort pulses, UWB indoor signals experience frequency-selective fading during transmission. The propagation model of the indoor wireless channel can be described by the impulse response of the channel as [3]

$$h(t) = \sum_{l=1}^{L} a_l(t) \delta(t - \tau_l(t)), \quad (5)$$

where t is the observation time, L is the number of the resolvable paths, $\tau_l(t)$ is the arrival-time of the received signal via the lth path which is log-normal distributed [5], $a_l(t)$ is the random time-varying amplitude attenuation, and δ denotes the Dirac delta function. Without loss of generality, we define $\tau_l(t)$ so that $\tau_1 < \tau_2 < \cdots < \tau_L$. For narrowband systems, the number of scatterers within one resolvable path is large, so that the central limit theorem can be applied, leading to a Gaussian model for the channel impulse response. However, UWB systems can resolve paths with a nanosecond path delay difference, hence the number of scatterers within one resolvable path is only on the order of 2 or 3 [3]. Since the number of scatterers is too small to apply the central limit theorem, the distribution of $a_l(t)$ cannot be modeled as Gaussian. Although the exact distribution of

$a_l(t)$ is difficult to derive, several models have been proposed [2, 3] considering that a small number of scatterers best describes the indoor wireless channel. In [2], the so-called POCA-NAZU model is introduced to describe the small scale multipath fading amplitudes for UWB signals, while [3] derives a STDL propagation model from experimental data. It is shown in [3] that the Nakagami distribution is the best fit for the indoor small-scale magnitude statistics.

We first write $a_l(t)$ as

$$a_l(t) = v_l a_l, \tag{6}$$

where $v_l = \text{sign}(a_l)$ and $a_l = |a_l(t)|$. The PDF of the amplitude of a_l is given by [3]

$$p(a_l) = \frac{2}{\Gamma(m)}\left(\frac{m}{\Omega_l}\right)^m a_l^{2m-1} e^{-ma_l^2/\Omega_l}, \tag{7}$$

where $\Gamma()$ denotes the Gamma function, $\Omega_l = E[a_l^2]$, and $m = [E[a_l^2]]^2/\text{Var}[a_l^2]$, which is a function of l and $m \geq 1/2$. Note that $a_l \geq 0$. As $\tau_1 < \tau_2 < \cdots < \tau_L$, it is reasonable to assume that the power of a_l is exponentially decreasing with increasing delay. To make the channel characteristics analyzable without affecting the generality of the channel, we further define v_l as a random variable that takes the values $+1$ or -1 with equal probability, and τ_l as a deterministic constant within the resolvable path time interval defined by $\tau_l = (l-1)\tau$ [11], where $\tau = 1/W$ and W is the signal bandwidth.

3. CAPACITY ANALYSIS WITH A SINGLE USER

3.1. Equivalent SNR

With a single user active in the system, (4) can be simplified to

$$r(t) = \sum_{l=1}^{L} a_l(t)\delta(t - \tau_l(t))X(t) + w(t), \tag{8}$$

where $X(t) = (s(t))' = \sum_{j=-\infty}^{\infty} A_{d_{\lfloor j/N_s \rfloor}} p(t - jT_f - c_j T_c - \delta_{d_{\lfloor j/N_s \rfloor}})$. The equivalent SNR of (8) is given by

$$\gamma = \frac{\int_{w/2}^{w/2} G_X(f)|H(f)|^2 df}{N_0 W}, \tag{9}$$

where $G_X(f)$ is the power spectral density (PSD) of the UWB signal determined by the pulse shape and modulation scheme, and $H(f)$ is the PSD of $h(t)$ given by $H(f) = \sum_{l=1}^{L} v_l a_l e^{-j2\pi f(l-1)\tau}$. Thus we have

$$|H(f)|^2 = \left(\sum_{l=1}^{L} v_l a_l \cos(2\pi f(l-1)\tau)\right)^2 + \left(\sum_{l=1}^{L} v_l a_l \sin(2\pi f(l-1)\tau)\right)^2. \tag{10}$$

The equivalent SNR γ can be written as

$$\gamma = \frac{\int_{w/2}^{w/2} G_X(f)[\alpha + \beta]df}{N_0 W}, \tag{11}$$

where α denotes $(\sum_{l=1}^{L} v_l a_l \cos(2\pi f(l-1)\tau))^2$ and β denotes $(\sum_{l=1}^{L} v_l a_l \sin(2\pi f(l-1)\tau))^2$.

Without loss of generality, we assume $X(t)$ has a uniformly distributed PSD to simplify the analysis, that is,

$$G_X(f) = \begin{cases} \dfrac{P_x}{W} & \text{where } f \in \left[-\dfrac{W}{2} \quad \dfrac{W}{2}\right], \\ 0 & \text{otherwise,} \end{cases} \tag{12}$$

where P_x is the power of the received UWB signal. Equation (11) can then be written as

$$\gamma = \gamma_s \frac{1}{\pi}\int_0^{\pi}\left[\left(\sum_{l=1}^{L} v_l a_l \cos((l-1)u)\right)^2 + \left(\sum_{l=1}^{L} v_l a_l \sin((l-1)u)\right)^2\right]du, \tag{13}$$

where $\gamma_s = P_X/WN_0$ is the symbol SNR of the UWB system. This shows that the equivalent SNR γ can be denoted by the symbol SNR modified according to the number of paths and the fading coefficients.

3.2. Capacity for frequency-selective fading channels

In general, the channel capacity is a function of the channel realization, transmitted signal power, and noise. As UWB communication is via ultrashort pulses, it is reasonable to assume that the channel is essentially fixed during one pulse duration. With this quasistatic assumption, the instantaneous capacity over frequency-selective fading channels can be calculated using the equivalent SNR in (13). The normalized capacity with respect to the bandwidth can then be obtained by averaging the instantaneous capacity over the PDF of the random time-varying amplitude attenuation vector **a**:

$$\begin{aligned}\overline{C} &= \int_0^{\infty} \log_2(1+\gamma)p(\mathbf{a})d\mathbf{a} \\ &= \int_0^{\infty}\cdots\int_0^{\infty} \log_2\left(1 + \gamma_s \frac{1}{\pi}\int_0^{\pi}\left[\left(\sum_{l=1}^{L} v_l a_l \cos((l-1)u)\right)^2 + \left(\sum_{l=1}^{L} v_l a_l \sin((l-1)u)\right)^2\right]du\right) \\ &\quad \times \prod_{l=1}^{L} p(a_l)da_1\, da_2 \cdots da_L.\end{aligned} \tag{14}$$

For frequency-selective fading, $L > 1$ and (14) will be evaluated via Monte Carlo simulation since it is difficult to derive a simple closed form expression. Although (14)

is calculated based on a specific pulse shape, the standard capacity expression has continuous inputs and continuous outputs. Therefore considering this restriction, (14) does not represent the exact channel capacity, but it does provide guidance and a means of comparison from the capacity perspective.

Note that frequency flat fading is also covered by (14) using $L = 1$, and this can be expressed in closed form after some simple manipulations as shown in Appendix A:

$$\begin{aligned}\overline{C} &= \frac{1}{\Gamma(m)}\int_0^\infty \log_2\left(1+\frac{u}{\rho}\right)u^{m-1}e^{-u}du \\ &= \frac{\rho^m}{\Gamma(m)}(\log_2 e) f\left(\frac{1}{\rho}, m-1\right),\end{aligned} \tag{15}$$

where $\rho = m/\Omega\gamma_s$, and

$$\begin{aligned}f(\overline{\gamma}_c, n) &= \int_0^\infty \ln(1+\gamma_s)\gamma_s^n e^{-\gamma_s/\overline{\gamma}_c}d\gamma_s \\ &= (-1)^{n-1}\overline{\gamma}_c e^{1/\gamma_c}\mathbf{Ei}\left(-\frac{1}{\gamma_c}\right) + \sum_{k=1}^{n}\frac{n!}{(n-k)!} \\ &\quad\times\left[\sum_{j=0}^{k}\sum_{i=0}^{k-j-1}\frac{(-1)^{n-k}}{(k-j-1-i)!}\frac{1}{(k-j)}\overline{\gamma}_c^{i+j+2}\right. \\ &\quad\left.+(-1)^{n-k-1}\overline{\gamma}_c^{k+1}e^{1/\gamma_c}\mathbf{Ei}\left(-\frac{1}{\overline{\gamma}_c}\right)\right]\end{aligned} \tag{16}$$

as described in [12].

3.3. Channel capacity for UWB PPM and PAM over frequency-selective fading channels

A channel with PPM or PAM modulation has discrete-valued inputs and continuous-valued outputs, which imposes an additional constraint on the capacity calculation. Directly applying the capacity formula in [9] by replacing the SNR with the equivalent SNR γ in (13), and then averaging over the joint pdf of $a_1 a_2 \cdots a_L$, the channel capacity for an M-ary PPM UWB system over a frequency-selective channel is given by

$$\begin{aligned}&C_{M-\mathrm{PPM}} \\ &= \iint_0^\infty \cdots \int_0^\infty \left\{\log_2 M - \mathrm{E}_v\left\{\log_2\sum_{i=1}^{M}\exp\left[\sqrt{\gamma}(v_i - v_1)\right]\right\}\right\} \\ &\quad\times\prod_{l=1}^{L}p(a_l)da_1 da_2\cdots da_L \text{ bits/channel use},\end{aligned} \tag{17}$$

where v_i, $i = 2, \ldots, M$ and v_1 are Gaussian random variables with distributions $N(0,1)$ and $N(\sqrt{\gamma}, 1)$, respectively. The expression $N(x,1)$ denotes a Gaussian distribution with mean x and variance 1. Monte Carlo simulation can be applied to (17) to evaluate the channel capacity of a UWB PPM system over frequency-selective channels.

Similarly, the channel capacity for an M-ary PAM UWB system over a frequency-selective channel can be written as

$$\begin{aligned}C_{M-\mathrm{PAM}} &= \iint_0^\infty \cdots \int_0^\infty \left\{\log_2 M - \frac{1}{M}\sum_{k=0}^{M-1}\mathrm{E}\right. \\ &\quad\left.\times\left\{\log_2\sum_{i=0}^{M-1}\exp\left[\gamma\left(|w|^2 - |s_k + w - s_i|^2\right)\right]\right\}\right\} \\ &\quad\times\prod_{l=1}^{L}p(a_l)da_1 da_2\cdots da_L,\end{aligned} \tag{18}$$

where $s_i = (2m - 1 - M)\sqrt{E_g}$ is one of the normalized M-ary PAM signals, and w is AWGN with zero mean and variance 1 in each real dimension.

3.4. Channel capacity of PPM or PAM UWB systems under FCC part 15 rules

Due to the possibility of interference to other communication systems by the ultra-wideband impulses, UWB is currently only allowed emission on an unlicensed basis subject to FCC part 15 rules which restricts the field strength to $E = 500$ microvolts/meter/MHz at a distance of $3m$. Thus the transmitted power constraint for a UWB system with a 1 GHz bandwidth is $P_t \leq -11$ dBm. The following relationship is obtained using a common link budget approach:

$$\frac{\gamma}{G} \leq -11\,\mathrm{dBm} - N_{\mathrm{thermal}} - F - 10\log\frac{(4\pi d)^n}{\lambda}, \tag{19}$$

where $G = N_s T_f W_p$ is the equivalent processing gain, W_p is the bandwidth of the UWB impulse related to the pulse duration Tp, N_{thermal} is the thermal noise floor, calculated as the product of Boltzmann's constant, room temperature (typically 300 K), noise figure, and bandwidth. F is the noise figure, λ is the wavelength corresponding to the center frequency of the pulse, and n is the path loss exponent. It is easily shown that the maximum reliable communication distance is determined primarily by the signal-to-noise ratio γ. Based on (17), (18), and (19), the maximum distance for reliable transmission of a PPM or PAM UWB system can be calculated. The relationship between system capacity and communication range will be demonstrated in Section 5.

3.5. Channel capacity over frequency-selective fading channels with a Rake receiver

A Rake receiver processes the received signal in an optimum manner if the receiver has perfect channel state information. The equivalent SNR for a Rake receiver is derived in Appendix B as

$$\begin{aligned}&\gamma_L \\ &= \gamma_s\frac{\int_0^\pi\left[\left(\sum_{l=1}^{L}a_l^2\cos((l-1)u)\right)^2 + \left(\sum_{l=1}^{L}a_l^2\sin((l-1)u)\right)^2\right]du}{\int_0^\pi\left[\left(\sum_{l=1}^{L}\nu_l a_l\cos((l-1)u)\right)^2 + \left(\sum_{l=1}^{L}\nu_l a_l\sin((l-1)u)\right)^2\right]du}.\end{aligned} \tag{20}$$

The equivalent SNR, γ_L, can be substituted into (17) and (18) and then averaged over the PDF of a_l to obtain the corresponding capacity with L-order receive diversity.

4. CAPACITY ANALYSIS OF A TIME-HOPPING MULTIPLE ACCESS PPM OR PAM UWB SYSTEM

With more than one user active in the system, multiaccess interference (MAI) is a major factor limiting performance and capacity, particularly for a large number of users. As shown in [8, 9], the net effect of the multiple-access interference produced by the undesired users at the output of the desired user's correlation receiver can be modeled as a zero-mean Gaussian random variable by invoking the central limit theorem. This allows the capacity analysis given in Section 3 for a single user to be extended to a multiple-access system.

4.1. Multiple-access interference model

As given in (4), the received signal is modeled as

$$r(t) = \sum_{k=1}^{K} \sum_{l=1}^{L} a_{lk}(t) X_l^{(k)}(t - \tau_{lk}) + w(t). \tag{21}$$

To evaluate the average SNR over the time-hopping sequences and propagation delays, we make the following reasonable assumptions to simplify the analysis.

(a) $X_l^{(k)}(t - \tau_{lk})$, for $k = 1, 2, \ldots, k$, where K is the number of active users, and the noise $n(t)$, are all assumed to be independent.
(b) The time-hopping sequences $c_j^{(k)}$ are assumed to be independent, identically distributed (i.i.d) random variables uniformly distributed over the time interval $[\theta, N_h]$.
(c) For simplicity and without loss of generality, we assume that each information symbol only uses a single UWB pulse, that is, $N_s = 1$. Results for other values of Ns can easily be obtained.
(d) All M-ary PPM or PAM signals are equally likely *a priori*.
(e) The time delays τ_{lk} are assumed to be i.i.d uniformly distributed over $[\theta, T_f]$.
(f) Perfect synchronization and channel equalization are assumed at the receiver, that is, τ_{lk} is known at the receiver.

We assume the desired user corresponds to $k = 1$. The basis functions of the N cross-correlators of the correlation receiver for user 1 are

$$u_s^{(l1)}(t) = a_{l1}^*(t) p(t - \delta_{s1} - \tau_{l1}), \quad s = 1, \ldots, N. \tag{22}$$

The outputs of each cross-correlator at the sample time $t = qT_f$ are

$$\hat{r}_s = \int_{(q-1)T_f}^{qT_f} r(t) u_s^{(l1)}(t - jT_f - c_j^{(1)} T_c)\, dt, \quad s = 1, \ldots, N. \tag{23}$$

Assuming PPM or PAM signal s_m is transmitted by user 1, (22) can be written in the form

$$\hat{r}_s = \begin{cases} \sum_{l=1}^{L} |a_{l1}|^2 A_m{}^{(1)} + W_{\mathrm{MAI}} + W, & s = m, \\ W_{\mathrm{MAI}} + W, & s \neq m, \end{cases} \tag{24}$$

where

$$\begin{aligned} W_{\mathrm{MAI}} &= \sum_{l=1}^{L} \int_{(p-1)T_f}^{pT_f} \sum_{k=2}^{K} a_{l1}^*(t) X^{(k)}(t - \tau_{lk}) \\ &\qquad \times p(t - \delta_{s1} - \tau_{l1} - jT_f - c_j^{(1)} T_c)\, dt \\ &= \sum_{l=1}^{L} \sum_{k=2}^{L} \int_{(p-1)T_f}^{pT_f} a_{l1}^*(t) A^{(k)} \\ &\qquad \times p(t - jT_f - c_j^{(k)} T_c - \delta_{d_j^{(k)}} - \tau_{lk}) \\ &\qquad \times p(t - \delta_{s1} - \tau_{l1} - jT_f - c_j^{(1)} T_c)\, dt \end{aligned} \tag{25}$$

is the MAI component and

$$W = \sum_{l=1}^{L} \int_{(p-1)T_f}^{pT_f} a_{l1}^*(t) w(t) p(t - \delta_{s1} - \tau_{l1} - jT_f - c_j^{(1)} T_c)\, dt \tag{26}$$

is the AWGN component.

By defining the autocorrelation function of $p(t)$ as

$$\theta(\Delta) = \int_0^{T_f} p(t) p(t - \Delta)\, dt, \tag{27}$$

and given the fact that $a_l(t) := v_l a_l$ is independent with $p(t)$ and, for practical purposes, can be viewed as independent with respect to t, (25) can be written as

$$W_{\mathrm{MAI}} = \sum_{l=1}^{L} \sum_{k=2}^{K} v_{lk} a_{lk} A^{(k)} \theta(\Delta), \tag{28}$$

where $\Delta = (c_j^{(1)} - c_j^{(k)}) T_c - (\delta_{s1} - \delta_{d_j^{(k)}}) - (\tau_{l1} - \tau_{lk})$ is the time difference between user 1 and user k. Under the assumptions listed above, Δ can be modeled as a random variable uniformly distributed over $[-T_f, T_f]$. With the Gaussian approximation, we require the mean and variance of (28) to characterize the output of the cross-correlators. Note that although a Gaussian approximation for the MAI of a UWB time-hopping PPM system may not always be accurate [13], it can still be used to provide meaningful results that are useful for comparison purposes.

It is easy to show that the AWGN component has mean zero and variance $\sum_{l=1}^{L} a_{l1}{}^2 N_0$. However, the mean and variance of the MAI component are determined by the specific pulse waveform. From the PSD given by (12), the autocorrelation function of the pulse is

$$\theta(\Delta) = \frac{\sin(W\Delta/2)}{\pi\Delta} \frac{P_x}{2\pi W}. \tag{29}$$

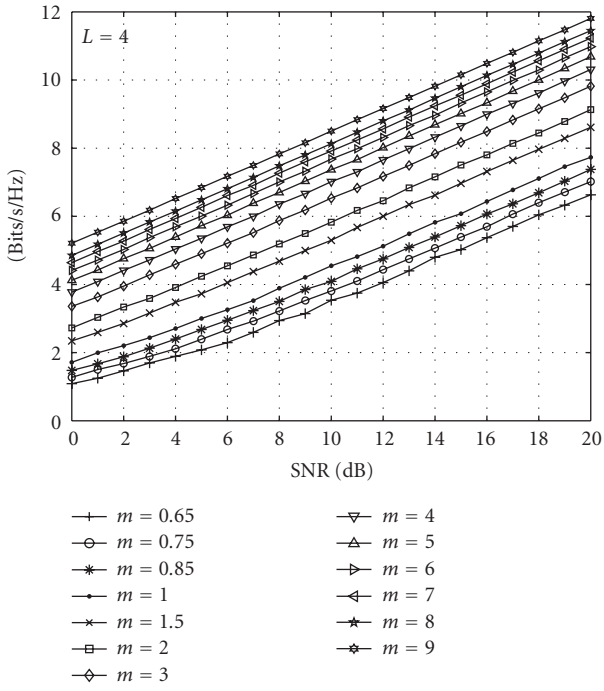

Figure 1: UWB multipath fading channel capacity with $L = 4$.

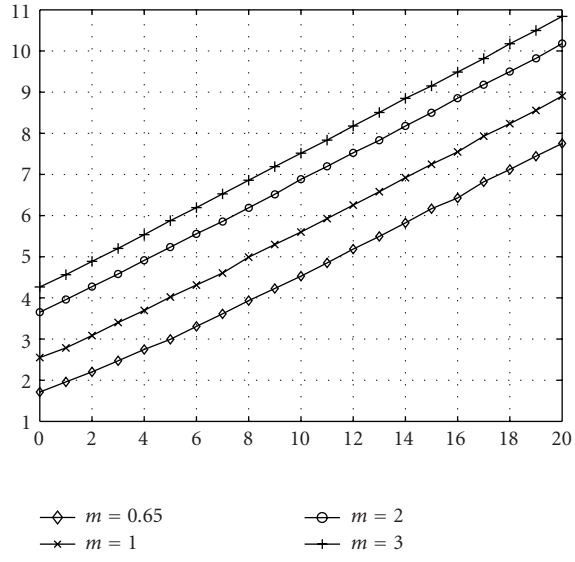

Figure 2: UWB multipath fading channel capacity with $L = 10$.

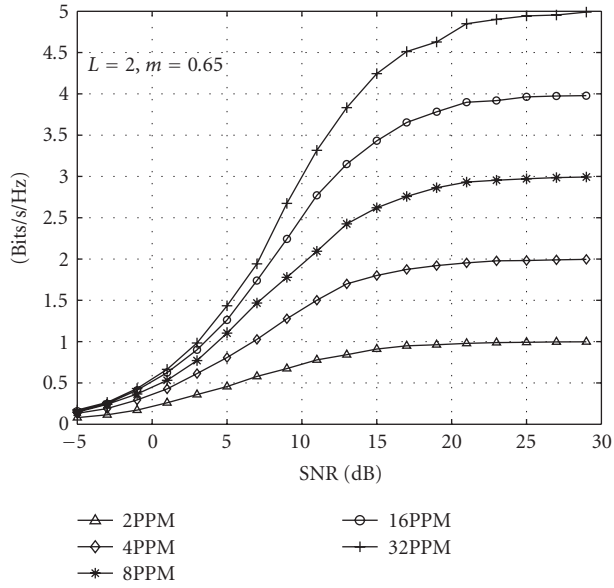

Figure 3: Capacity of a UWB system with PPM over a multipath fading channel with $L = 2$ and $m = 0.65$.

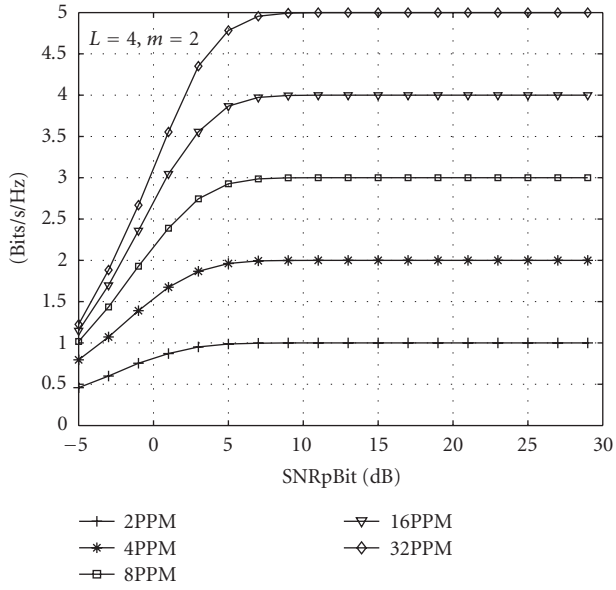

Figure 4: Capacity of a UWB system with PPM over a multipath fading channel with $L = 4$ and $m = 2$.

From (29), the mean of W_{MAI} can then be calculated as

$$E[W_{\mathrm{MAI}}] = E\left[\sum_{l=1}^{L}\sum_{k=2}^{K} v_{lk}a_{lk}A^{(k)}\theta(\Delta)\right] = \sum_{l=1}^{L}\sum_{k=2}^{K} E[v_{lk}]E[a_{lk}A^{(k)}]E[\theta(\Delta)] = 0 \tag{30}$$

and the variance of W_{MAI} is

$$\mathrm{Var}[W_{\mathrm{MAI}}] = \mathrm{Var}\left[\sum_{l=1}^{L}\sum_{k=2}^{K} v_{lk}a_{lk}A^{(k)}\theta(\Delta)\right] = \sum_{l=1}^{L}\sum_{k=2}^{K} E\left(a_{lk}A^{(k)}\right)^2 E[\theta^2(\Delta)]. \tag{31}$$

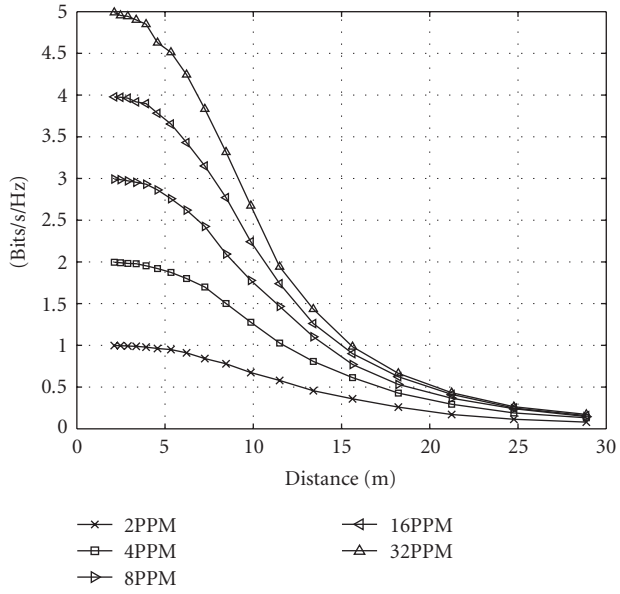

Figure 5: Relationship between distance and channel capacity of a UWB system with PPM over a multipath fading channel, $L = 2$, $m = 0.65$, and $n = 3$.

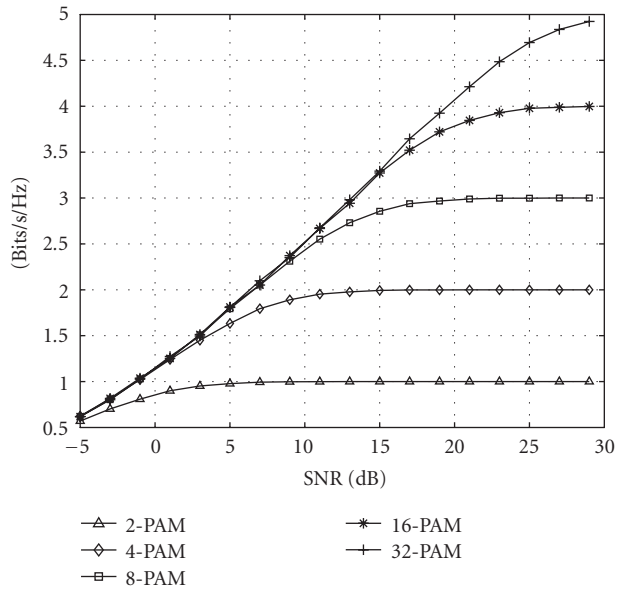

Figure 6: Capacity of a UWB system with PAM over a multipath fading channel with $L = 4$ and $m = 0.65$.

Given that

$$E[\theta^2(\Delta)] = E\left[\frac{\sin^2(W\Delta/2)}{(\pi\Delta)^2}\left(\frac{P_x}{2\pi W}\right)^2\right] = \left(\frac{P_x}{2\pi W}\right)^2 \int_{-T_f}^{T_f} \frac{\sin^2(W\Delta/2)}{(\pi\Delta)^2}\frac{1}{2T_f}d\Delta \approx \left(\frac{P_x}{2\pi W}\right)^2 \frac{1}{\pi^2}\frac{1}{2T_f}\frac{\pi}{2}\frac{W}{2} = \frac{P_x^2}{32G\pi^3}, \quad (32)$$

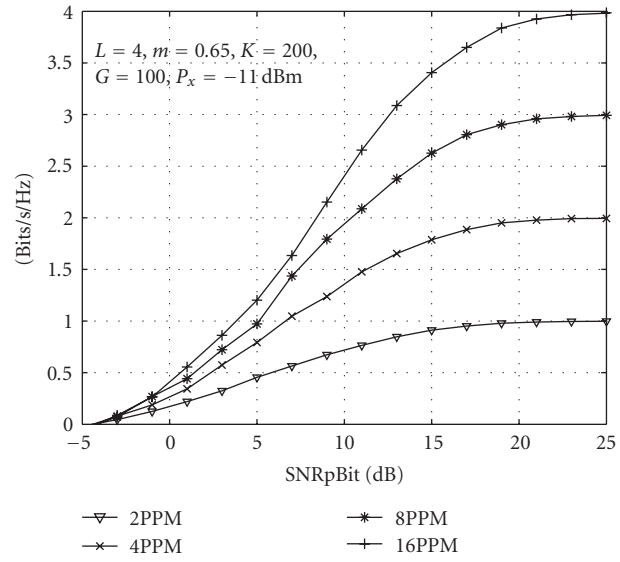

Figure 7: Capacity of a multiple access UWB system with PPM over a multipath fading channel with $L = 4$, $m = 0.65$, $K = 200$, $G = 100$, and $P_x = -11$ dBm.

we can write the variance as

$$\sigma_{\mathrm{MAI}} = \mathrm{Var}[W_{\mathrm{MAI}}] = \sum_{l=1}^{L}\sum_{k=2}^{K}\frac{a_{lk}^2 P_x^2}{32G\pi^3}E_g, \quad (33)$$

where $G = T_f/T_p$ is the processing gain of the UWB system.

Note that the approximation in (32) is based on the fact that most of the energy of the Sinc function is located in $[-T_f, T_f]$. Hence the cross-correlator outputs of user 1's receiver can be modeled as independent Gaussian random variables with distributions

$$\hat{r}_j \sim N\left(\sum_{l=1}^{L}|a_{l1}|^2 A_m{}^{(1)}\sqrt{E_g}, \sigma_{\mathrm{total}}^2\right), \quad j = n, \qquad \hat{r}_j \sim N(0, \sigma_{\mathrm{total}}^2), \quad j \neq n, \quad (34)$$

where $\sigma_{\mathrm{total}}^2 = \sum_{l=1}^{L}\sum_{k=2}^{K}(a_{lk}^2 P_x^2/32G\pi^3)E_g + \sum_{l=1}^{L} a_{l1}{}^2 N_0$.

The equivalent SNR is

$$\gamma = \frac{\left(\sum_{l=1}^{L}|a_{l1}|^2 A_m{}^{(1)}\right)^2 E_g}{\sum_{l=1}^{L}\sum_{k=2}^{K}(a_{lk}^2 P_x^2/32G\pi^3)E_g + \sum_{l=1}^{L} a_{l1}{}^2 N_0}, \quad (35)$$

which can be written as

$$\gamma = \frac{\left(\sum_{l=1}^{L}|a_{l1}|^2\right)^2}{\sum_{l=1}^{L}\sum_{k=2}^{K}(a_{lk}^2 P_x^2/32G\pi^3) + \sum_{l=1}^{L}(a_{l1}{}^2/\mathrm{SNR})}, \qquad \gamma = \frac{\left(\sum_{l=1}^{L}|a_{l1}|^2\right)^2 (3/(M^2-1))}{\sum_{l=1}^{L}\sum_{k=2}^{K}(a_{lk}^2 P_x^2/32G\pi^3) + \sum_{l=1}^{L}(a_{l1}{}^2/\mathrm{SNR})} \quad (36)$$

for PPM and PAM, respectively.

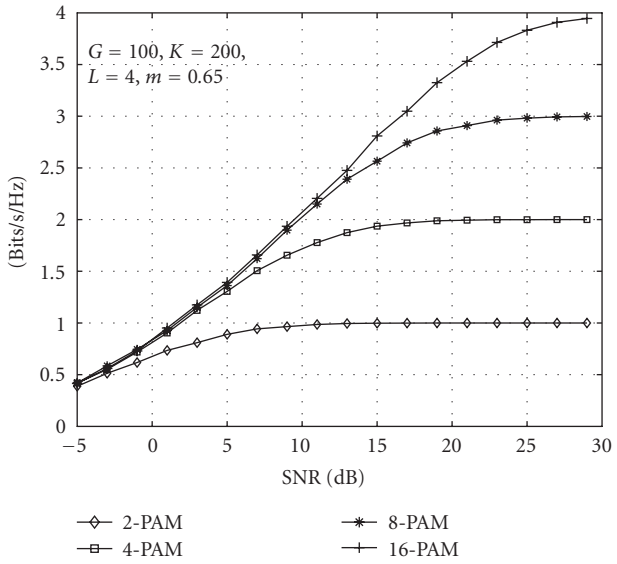

Figure 8: Capacity of a multiple access UWB system with PAM over a multipath fading channel with $L = 4$, $m = 0.65$, $K = 200$, $G = 100$, and $P_x = -11$ dBm.

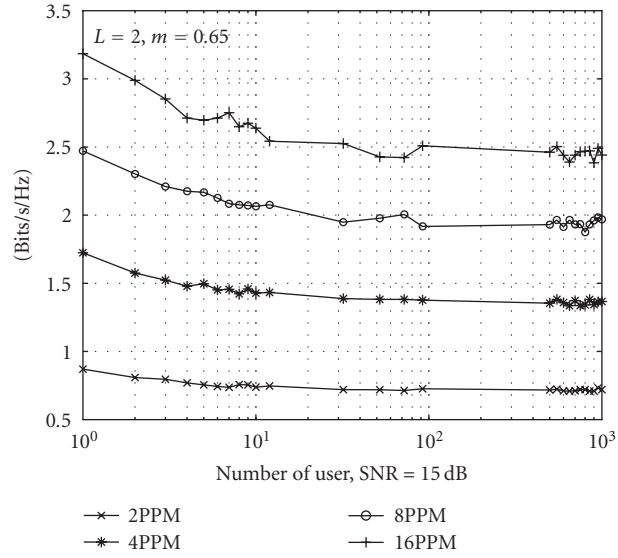

Figure 9: Relationship between channel capacity and number of users for a multiple access UWB system with PPM over a multipath fading channel, $L = 2$, $m = 0.65$, $G = 100$, $P_x = -11$ dBm, and SNR = 15 dB.

The instantaneous capacity for a multiple access UWB system with PPM or PAM can be obtained by substituting γ from (35) in (17) or (18), respectively. The channel capacity can then be obtained by averaging the instantaneous capacities over the joint PDF of a_l.

5. NUMERICAL RESULTS

In this section, some numerical results are presented to illustrate and verify the analytical expressions obtained previously.

Figures 1 and 2 show the capacity of the multipath fading UWB channel with continuous inputs and outputs with $L = 2$ and $L = 4$, respectively. This shows that the capacity increases as m increases, and $L = 4$ can achieve a higher capacity than $L = 2$ for the same SNR. Note that the capacity for $L = 4$ is almost equal to the $1.5m$, $L = 2$ capacity.

Figure 3 shows the capacity of a UWB system with PPM over multipath fading channels, with $L = 2$ and $m = 0.65$, while Figure 4 gives the capacity for $L = 4$ and $m = 2$. Obviously, the larger L and m, the greater the capacity.

Figure 5 presents the relationship between reliable channel capacity and the communication range subject to FCC Part 15 rules. The link budget model in (18) is applied and the channel parameters are $n = 3$, $L = 2$, and $m = 0.65$. This shows that PPM can provide full capacity only within $2m$ in most cases. However, less than half of the capacity can be achieved when the communication distance is extended to $10m$ over a fading channel. In general, a UWB system can only provide reliable transmission over very short or medium ranges with the restriction of FCC Part 15 rules and a multipath fading channel.

Figure 6 shows the capacity of PAM over a multipath fading channel with $L = 4$ and $m = 0.65$. The capacity of a multiple access UWB system with PPM and PAM over a multipath fading channel with $L = 4$, $m = 0.65$, $K = 200$, $G = 100$, and $P_x = -11$ dBm is shown in Figures 7 and 8, respectively. The relationship between the number of users and the capacity of a PPM UWB system is demonstrated in Figure 9. This shows that the system can only achieve less than half the capacity with 10 simultaneous active users.

6. CONCLUSIONS

The capacity of UWB PPM and PAM systems over multipath fading channels has been studied from a SNR perspective. The capacity was first derived for an AWGN channel and then extended to a fading channel by averaging the SNR over the channel random variables. Both single and multiple user capacities were considered. Exact capacity expressions were derived, and Monte Carlo simulation was employed for efficient evaluation. It was shown that fading has a significant effect on the capacity of a UWB system.

APPENDICES

A. CAPACITY OVER FLAT FADING CHANNEL

The channel capacity for a UWB system in a flat fading channel can be obtained by letting $L = 1$ in (14):

$$\overline{C} = \int_0^\infty \log_2(1 + \gamma_s a_1^2)\, p(a_1)\, da_1$$

$$= \int_0^\infty \log_2(1 + \gamma_s a_1^2)\, \frac{2}{\Gamma(m)} \left(\frac{m}{\Omega_1}\right)^m a_1^{2m-1} e^{-m a_1^2/\Omega_1}\, da_1. \tag{A.1}$$

To simplify the expression, we substitute $u = (m/\Omega)a^2$, so that (A.1) can be written as

$$\overline{C} = \frac{1}{\Gamma(m)} \int_0^\infty \log_2\left(1 + \frac{\Omega\gamma_s}{m}u\right) u^{m-1} e^{-u}\, du. \tag{A.2}$$

By letting $\rho = m/\Omega\gamma_s$, (A.2) can be simplified to

$$\overline{C} = \frac{1}{\Gamma(m)} \int_0^\infty \log_2\left(1 + \frac{u}{\rho}\right) u^{m-1} e^{-u}\, du. \tag{A.3}$$

B. EQUIVALENT SNR FOR A RAKE RECEIVER OVER FREQUENCY-SELECTIVE FADING CHANNELS

A Rake receiver will process the received signal in an optimum manner if the receiver has perfect channel state information. The received signal (4) can then be written as

$$r(t) = \sum_{l=1}^{L} a_l^2 \delta(t - \tau_l(t)) X(t) + \sum_{l=1}^{L} a_l^*(t) \delta(t - \tau_l(t)) w(t). \tag{B.1}$$

The equivalent SNR of (B.1) is given by

$$\gamma_L = \frac{\int_{w/2}^{w/2} G_X(f) \left| \sum_{l=1}^{L} a_l^2 e^{-j2\pi f(l-1)\tau} \right|^2 df}{\int_{w/2}^{w/2} G_W(f) \left| \sum_{l=1}^{L} v_l a_l e^{-j2\pi f(l-1)\tau} \right|^2 df}. \tag{B.2}$$

Note that $G_X(f)$ is defined in (12), and

$$G_W(f) = \begin{cases} N_0, & \text{where } f \in \left[-\dfrac{W}{2} \quad \dfrac{W}{2}\right] \\ 0, & \text{otherwise.} \end{cases} \tag{B.3}$$

Equation (B.2) can then be written as

$$\gamma_L = \gamma_s \frac{\int_0^\pi \left[\left(\sum_{l=1}^{L} a_l^2 \cos((l-1)u)\right)^2 + \left(\sum_{l=1}^{L} a_l^2 \sin((l-1)u)\right)^2\right] du}{\int_0^\pi \left[\left(\sum_{l=1}^{L} v_l a_l \cos((l-1)u)\right)^2 + \left(\sum_{l=1}^{L} v_l a_l \sin((l-1)u)\right)^2\right] du}. \tag{B.4}$$

ACKNOWLEDGMENTS

This work is supported by National 863 Hi-Tech Research and Development Program of China under Grant no. 2007AA12Z317 and Science & Technology Developing Program of Qingdao, China under Grant 06-2-3-19-gaoxiao.

REFERENCES

[1] M. Z. Win and R. A. Scholtz, "Ultra-wide bandwidth time-hopping spread-spectrum impulse radio for wireless multiple-access communications," *IEEE Transactions on Communications*, vol. 48, no. 4, pp. 679–691, 2000.

[2] D. Cassioli, M. Z. Win, and A. F. Molisch, "The ultra-wide bandwidth indoor channel: from statistical model to simulations," *IEEE Journal on Selected Areas in Communications*, vol. 20, no. 6, pp. 1247–1257, 2002.

[3] H. Zhang, T. Udagawa, T. Arita, and M. Nakagawa, "A statistical model for the small-scale multipath fading characteristics of ultrawide band indoor channel," in *Proceedings of IEEE Conference on Ultra Wideband Systems and Technologies (UWBST '02)*, pp. 81–85, Baltimore, Md, USA, May 2002.

[4] A. F. Molisch, "IEEE 802.15.4a channel model—final report," IEEE 802.15-04-0662-00-004a, November 2004.

[5] L. Zhao and A. M. Haimovich, "Capacity of M-ary PPM ultra-wideband communications over AWGN channels," in *Proceedings of the 54th IEEE Vehicular Technology Conference (VTC '01)*, vol. 2, pp. 1191–1195, Atlantic City, NJ, USA, October 2001.

[6] L. Zhao and A. M. Haimovich, "The capacity of an UWB multiple-access communications system," in *Proceedings of IEEE International Conference on Communications (ICC '02)*, vol. 3, pp. 1964–1968, New York, NY, USA, April-May 2002.

[7] H. Zhang, W. Li, and T. A. Gulliver, "Pulse position amplitude modulation for time-hopping multiple-access UWB communications," *IEEE Transactions on Communications*, vol. 53, no. 8, pp. 1269–1273, 2005.

[8] H. Zhang and T. A. Gulliver, "Biorthogonal pulse position modulation for time-hopping multiple access UWB communications," *IEEE Transactions on Wireless Communications*, vol. 4, no. 3, pp. 1154–1162, 2005.

[9] H. Zhang and T. A. Gulliver, "Performance and capacity of PAM and PPM UWB time-hopping multiple access communications with receive diversity," *EURASIP Journal on Applied Signal Processing*, vol. 2005, no. 3, pp. 306–315, 2005.

[10] J. R. Foerster, "Ultra-wideband technology for short- or medium-range wireless communications," *Intel Technology Journal*, vol. 5, no. Q2, pp. 1–11, 2001.

[11] F. Zheng and T. Kaiser, "On the evaluation of channel capacity of multi-antenna UWB indoor wireless systems," in *Proceedings of IEEE International Symposium on Spread Spectrum Techniques and Applications (ISSSTA '04)*, pp. 525–529, Sydney, Australia, August-September 2004.

[12] H. Zhang and T. A. Gulliver, "Closed form capacity expressions for space time block codes over fading channels," in *Proceedings of IEEE International Symposium on Information Theory (ISIT '04)*, p. 411, Chicago, Il, USA, July 2004.

[13] G. Durisi and G. Romano, "On the validity of Gaussian approximation to characterize the multiuser capacity of UWB TH PPM," in *Proceedings of IEEE Conference on Ultra Wideband Systems and Technologies (UWBST '02)*, pp. 157–161, Baltimore, Md, USA, May 2002.